Best Student Paper Award 2nd Place

All-printed Multifunctional Sensors for Structural Health Monitoring of Inflatable Habitats

Matt Zuzelski[1], Isaac Little[1], Jun Zhuang[2], and Zhangxian Deng[1]

[1]Department of Mechanical and Biomedical Engineering, Boise State University, 1910 University Drive, Boise, ID 83725

[2]Computer Science Department, Boise State University, 1910 University Drive, Boise, ID 83725

Abstract

Inflatable structures present an efficient solution for deep space habitats, enabling compact storage during launch and providing a large operational volume once deployed in space. However, their lightweight and thin-walled design makes them susceptible to micro-meteoroids and orbital debris (MMODs), as well as the cumulative effects of creep strain. To ensure the safety of these inflatable habitats, this study used a commercial material extrusion system to prototype a flexible and multifunctional sensor for non-destructive structural health monitoring. This unique sensor consists of a piezoelectric polyvinylidene fluoride-trifluoroethylene (PVDF-trFE) film sandwiched between a pair of electrodes. The piezoelectric layer detects dynamic impact force due to MMODs and the electrodes printed into piezoresistive strain gauges are capable of measuring creep strain. In this study, a comprehensive sensor fabrication technique, including piezoelectric ink synthesis, printer settings, and material post-processing method, was first developed. Subsequent experiments using a mechanical load frame and impact hammer quantified the sensor sensitivity in piezoresistive and piezoelectric mode, respectively. The printed sensor achieved a gauge factor exceeding 8 in piezoresistive mode. An additional machine learning model predicted impact magnitude and impact width with linear correlation coefficients of 0.99 and 0.89, respectively, when compared to the tested values. These promising results underscore the potential for in-situ manufacturing of such multifunctional sensors, paving the way for sustainable deep space missions that not only minimize launch mass but also diminish reliance on exhaustive pre-launch designs.

Keywords— Additive Manufacturing, Material Extrusion, Piezoelectric, Piezoresistive, Inflatable Habitats

1 Introduction

Space habitats are essential environments that enable astronauts to perform daily activities and conduct research [1]. Inflatable habitats are a viable and efficient option, since they are lightweight and compact during launch while providing a large functional volume upon deployment in space. These inflatable habitats are constructed from flexible but high-strength thin-walled structures, also known as soft structural textiles (SSTs) [1]. A typical SST comprises three main components: an insulation layer, a pressurized bladder, and a restraint layer [2]. Monitoring the structural health of the restraint layer is crucial because it shoulders most of the structural load in inflatable structures and is vulnerable to micro-meteoroids and orbital debris (MMODs), in addition to the gradual impact of creep strain. Thus, integrating a broadband sensor that can detect both the high-frequency impact forces from MMODs and the low-frequency creep strain is essential. Installed at the restraint layer, this sensor is key for non-destructive and real-time structural health monitoring (SHM) of inflatable habitats, thereby ensuring the safety of the crew inside.

Given that the insulation layer can effectively shield the restraint layer from ionizing radiation and temperature fluctuations, traditional SHM systems like strain gauges, accelerometers, and piezoelectric force sensors, which are typically designed for benign lab environments, become viable options for use in inflatable habitats. Strain gauges that are ideal for low-frequency creep strain measurement are available in various designs, including piezoresistive and capacitive sensors [3, 4]. Piezoresistive strain gauges, in particular, are advantageous for inflatable structure SHM, as they can detect large strain while requiring relatively simple signal processing.

Impact detection has been performed with several methods including, but not limited to, broadband wave-based acoustic emission sensors, laser vibrometry, and piezoelectric thin films [5, 6, 7]. While these methods require skilled technicians and expensive technological supporting equipment, the piezoelectric thin film sensors are capable of high frequency

Health Monitoring of Structural and Biological Systems XVIII, edited by Zhongqing Su, Kara J. Peters, Fabrizio Ricci, Piervincenzo Rizzo, Proc. of SPIE Vol. 12951, 1295123 · © 2024 SPIE · 0277-786X · doi: 10.1117/12.3009977

impact detection with a relatively simple supporting system. Piezoelectric polymers, such as polyvinylidene fluoride-trifluoroethylene (PVDF-trFE), are of particular interest due to their biocompatibility, flexibility, and printability. These readily available polymers open the pathway for in-space, on-demand, rapid prototyping of complex sensor networks via additive manufacturing. Coupling the printable nature of PVDF-trFE thin films and silver ink piezoresistive strain gauges, an all-printed dual-sensor is made possible that effectively reduces the amount of fabrication required for SHM of the inflatable habitats without sacrificing sensing quality.

Additive manufacturing envelopes many techniques for generating a structure in a layer by layer fashion. Material extrusion (MEX) is one that involves controlled deposition of materials onto a target host structure with desired dimensions. This quality is highly beneficial to sensor prototyping as the installation is simplified without the need for glues or other clamping mechanisms. Recently, it has been shown that both piezoresistive and piezoelectric sensors can be printed via MEX [8, 9].

Leveraging the capabilities of advanced multi-material MEX systems (Hyrel 30M engine), this study achieved the co-printing of piezoelectric PVDF-trFE polymers and silver paste conductive traces, producing an integrated dual-mode sensor capable of detecting both high-frequency impacts and low-frequency creep strain simultaneously. Through experiments utilizing an impact hammer and a mechanical load frame, the sensor's sensitivity in both piezoelectric and piezoresistive modes was thoroughly evaluated. The outcomes of this research demonstrate the potential to construct highly sensitive, multifunctional, and flexible sensors within the restraint layer, facilitating in-situ and real-time SHM of inflatable habitats.

2 Sensor Fabrication

The dual-mode sensor consists of a meandering silver paste trace printed on a PVDF-trFE film. Pure Cu and Cu-coated Kapton are both used as substrates in this study, as shown in Figure 1. The silver paste conductive trace serves as a piezoresistive strain gauge, with its electrical impedance rising in tandem with mechanical strain. Impact events, on the other hand, generate surface charges on the PVDF-trFE film, which are detectable through the electrical voltage measured between the bottom copper electrode and the top silver paste electrode.

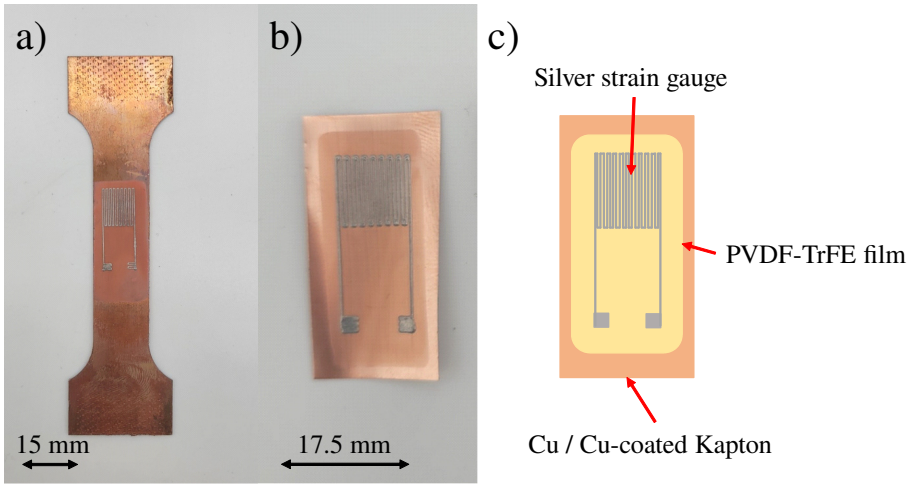

Figure 1: Dual-mode sensors featuring printed PVDF-trFE film and silver conductive traces printed on a) Cu dog bone and b) Cu-coated Kapton. c) Schematic of printed dual-mode sensor.

2.1 Material Extrusion

The dual-mode sensor was fabricated by co-printing a customized piezoelectric ink and a commercial silver paste on a Hyrel 30M engine (Hyrel 3D) as presented in Figure 2. The piezoelectric ink was formulated by dissolving 1.205 g of commercial PVDF-trFE powder (80/20 mol ratio, sourced from PolyK Technologies) in a co-solvent consisting of 1.830 g methyl ethyl ketone (MEK) and 5.000 g dimethyl sulfoxide (DMSO), both obtained from Sigma-Aldrich. This process resulted in a solution with a PVDF-trFE concentration of 15 wt.%. The PVDF-trFE ink was loaded into a 5 mL polypropylene syringe equipped with an 18-gauge luer-lock needle. After installing the syringe into the print head, a custom G-code

program was loaded to print films on the desired regions of the substrate. A preheated laboratory oven (FAITHFUL WHL-25AB) was used to dry the films at 90 °C for 1 hour. Immediately after drying, the films were annealed at 130 °C for 1 hour. The silver paste used in this study was sourced from Novacentrix (HPS-FG77 Silver Nanoflake Ink) due to its low curing temperature. Using a 5 mL polypropylene syringe and a 25-gauge luer-lock needle, a meandering conductive trace was printed on the PVDF-trFE film. After silver printing, the entire sensor was dried and cured in a furnace at 80 °C for 8 hours for silver paste curing. This low temperature effectively prevented unintentional depolarization of the piezoelectric film.

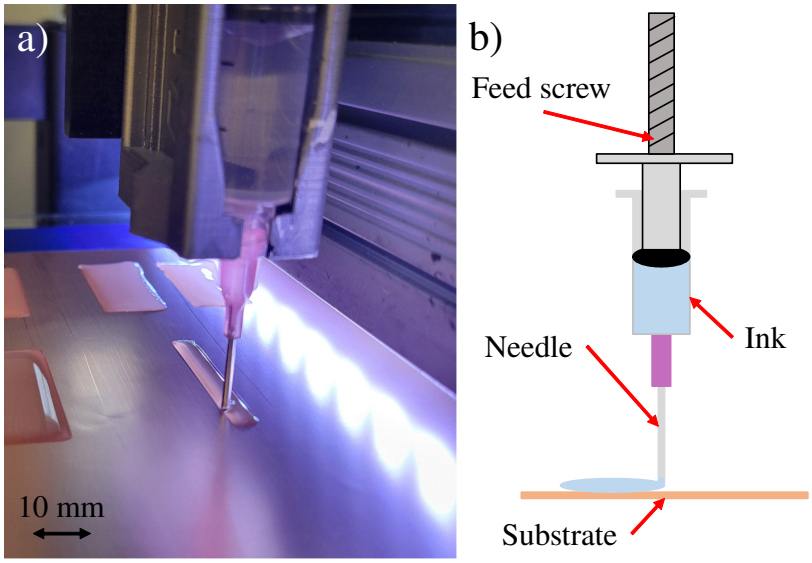

Figure 2: a) Physical assembly and b) schematic of the MEX system while printing PVDF-trFE films onto Cu-coated Kapton.

2.2 Piezoelectric Film Poling

PVDF-trFE film in β-phase exhibits a significant piezoelectric coefficient d_{33} of over 25 pC/N [10], however, as-printed PVDF-trFE film is mainly in α-phase featuring a weak piezoelectric coefficient d_{33}. In order to convert PVDF-trFE from α-phase to β-phase, the cured PVDF-trFE film was polarized using a customized corona poling rig, as shown in Figure 3. A voltage of -15 kV was applied to the tungsten needle for 3 minutes at room temperature, with the needle tip positioned 17 mm away from the film surface. This distance optimizes the poling process' effectiveness while accommodating a large area of the film. The tungsten needle was enclosed within a polylactic acid (PLA) tube sealed by a rubber O-ring. This configuration focused the ionized air produced at the needle, thereby enhancing the efficiency of corona poling. Given the extensive size of the film, the PVDF-trFE film underwent the corona poling process at three evenly spaced points along its central line to ensure uniform treatment.

2.3 Kevlar Strap Sensor Attachment

As a proof-of-concept, the sensor patch was affixed onto a Kevlar strap to demonstrate functionality on SSTs. A strain gauge adhesive (Omega TT300) was used to bond the printed sensor on the Kevlar strap. The adhesive was cured in a furnace at 80 °C for 5 hours. Following attachment to the Kevlar, the sensor was encapsulated in Polydimethylsiloxane (PDMS,Sylgard 184) to safeguard the silver traces from abrasion. While this attachment method works so far, the ultimate goal of this study is to remove the need for adhesives. One potential solution is to directly print a conductive ink (e.g., stretchable silver) on the Kevlar.

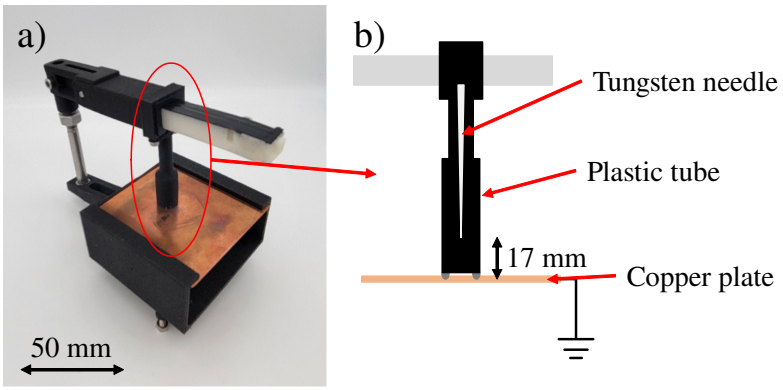

Figure 3: a) Physical assembly and b) schematic of customized corona poling rig for printed PVDF-trFE films.

3 Sensor Characterization

3.1 Low Frequency Strain Measurement

To evaluate the sensor's efficacy as a piezoresistive sensor, the dual-mode sensor was initially printed onto a Cu dog bone substrate. The experimental setup used for strain gauge testing is illustrated in Figure 4(a). A tensile load was applied using an MTS Criterion Model 43 load frame. To ensure quasi-static stretching, the load frame was programmed to pull the Cu dog bones at a speed of 0.01 mm/s up to a total 1.5 mm crosshead displacement. An electric impedance analyzer (Keysight E4990A) then recorded the electric resistance across the top meandering silver trace during the loading process. To facilitate sensor calibration, a digital image correlation (DIC) system (Correlated Solutions VIC-3D) was used to measure strain on the Cu dog bone sample. The other side of the dog bone sample was spray-painted with a white paint and speckle-coated using a speckle stamp. During the calibration process, meticulous attention was given to achieving a projection error of less than 0.1. Furthermore, when processing the images, no individual image exhibited a projection error exceeding 0.1.

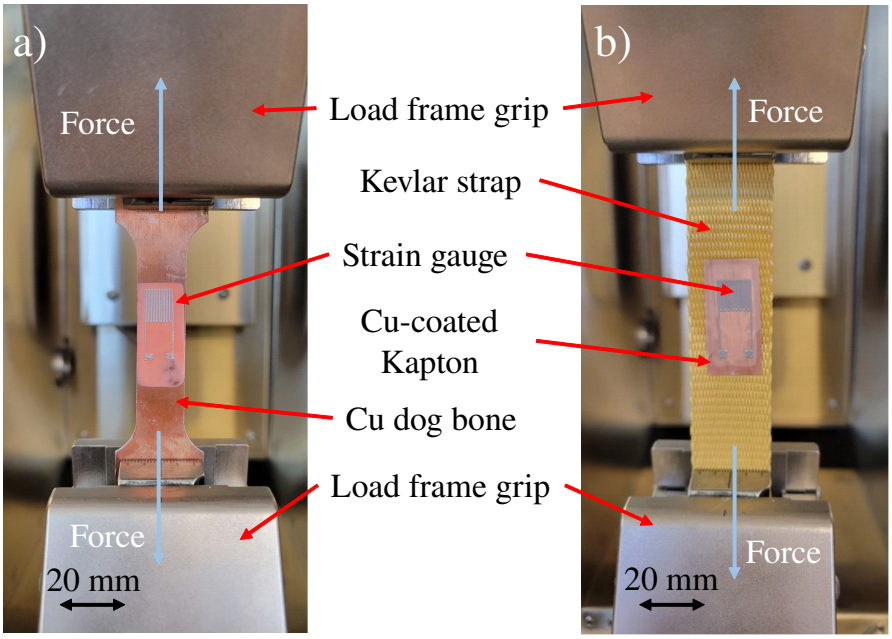

Figure 4: Sensor characterization setup for all-printed dual-mode sensors: (a) printed on Cu dogbone and (b) printed on Cu-coated Kapton and bonded to Kevlar strap.

3.2 High Frequency Impact Measurement

To evaluate the sensor's performance in piezoelectric mode, sensors were fabricated on both pure Cu and Cu-coated Kapton substrates. Both samples were subjected to a constant tension of 1 kN, as depicted in Figure 4. A commercial impact hammer (PCB Piezotronics 086C01) was employed to strike the Kevlar strap, while the force signal from the hammer was recorded by a LabVIEW data acquisition system. The electrical voltage generated across the top silver electrode and the bottom copper electrode was measured using the same LabVIEW system, ensuring accurate time synchronization. The sensor underwent impact testing in the piezoelectric mode 600 times, using an extender mass and a medium-stiffness plastic tip. Special attention was devoted to avoiding double hits with the impact hammer to prevent introducing unwanted variability into the data. A typical force measurement by the impact hammer and the corresponding voltage measurement from the sensor are presented in Figure 5.

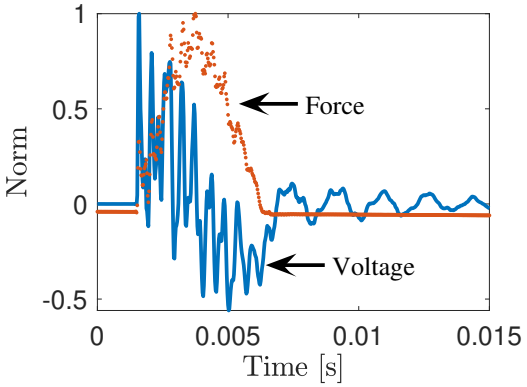

Figure 5: Force signal from impact hammer (orange and dotted line) and voltage signal from printed sensor (blue and solid line) after a typical impact hammer strike. Both signals were normalized to the maximum value.

By manually picking the amplitudes from both signals, the piezoelectric sensitivity S of the PVDF-trFE film impact sensor was found to be about 145 mV/N via Eq. 1

$$S = \frac{V_{max} - V_{min}}{F_{mag}}, \tag{1}$$

where V_{max} is the maximum recorded voltage, V_{min} is the minimum recorded voltage, and F_{mag} is the magnitude of the impact hammer force.

4 Results and Discussion

4.1 Piezoresistive Mode Results

The average strain ϵ within the surface area of the sensor was used for sensor validation. Additionally, the strain-induced resistance variance R_{var} was calculated via Eq. 2.

$$R_{var} = \frac{R(\epsilon) - R_0}{R_0}, \tag{2}$$

where $R(\epsilon)$ and R_0 are the electric resistance of the meandering silver trace at a given ϵ and zero strain, respectively. Figure 6 presents the resistance variance as a function of ϵ measured from three different sensors. Similar to other piezoresistive strain gauges based on particulate composites, all three sensors in this study exhibits two distinct linear regions [11, 12, 13, 8]. The first linear region at low strain (ϵ<0.5%) originates from the geometric change in conductive traces. Conversely, the subsequent linear region at high strain (ϵ>0.5%) stems from micro-structural changes, particularly alterations in the conductive pathways within the silver paste trace. Given that the creep strain anticipated in inflatable habitats far exceeds 1%, the practical deployment of this sensor may concentrate solely on its high-strain linear response region.

Table 1 quantifies the gauge factors (GFs) and linear correlation coefficients R^2 of three printed sensors. The sensor in piezoresistive mode exhibits multiple gauge factors from 1.41-3.68 in the low strain region and 5.64-8.02 in the high strain

region. Meanwhile, the linear correlation coefficient averages 0.93 and 0.99 for the low strain and high strain regions, respectively.

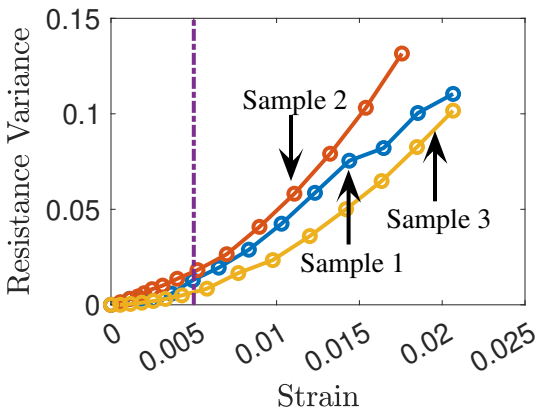

Figure 6: Performance of the printed sensor in piezoresistive mode. The purple dashed line separates the two linear regions.

Table 1: Gauge factor and linear correlation coefficient at different strain levels.

	Low Strain		High Strain	
Sensor	Gauge Factor	R^2	Gauge Factor	R^2
1	2.94	0.86	5.85	0.99
2	3.68	0.98	8.02	0.99
3	1.41	0.94	5.64	0.99

4.2 Piezoelectric Mode Results

A machine learning algorithm was employed to predict the impact magnitude and width using the voltage signal received from the piezoelectric film. The model was trained on a pre-processed dataset containing information on the magnitude, width, and voltage response for each impact. Subsequently, a new dataset was used to validate the model accuracy. The ultimate objective is for the model to accurately determine the impact magnitude and width solely based on the voltage response from the piezoelectric film. Not only would this allow for general detection of an impact event but, this would also allow detection of the amount of energy imparted on the structure by the orbital debris.

Impact test results with a force magnitude of over 10 N were used for machine learning model training to mitigate the impact of signal noises. For the sensor printed on a Cu dog bone substrate, a total of 410 impact datasets were gathered. Meanwhile, for the sensor printed on a Cu-coated Kapton substrate and affixed to the Kevlar strap, we collected a total of 117 impact datasets. In both cases, 80% of these datasets—328 impacts for the Cu dog bone sensor and 94 impacts for the Cu-coated Kapton sensor—were allocated for training the machine learning model. The remaining 20%—82 impacts for the Cu dog bone sensor and 23 impacts for the Cu-coated Kapton sensor—were reserved for testing the predictive capabilities of the model. Figure 7 compares the model predictions with experimental data for sensors printed and tested on rigid Cu dog bones. The accuracy of the model was measured by the linear correlation coefficient ρ^2. The predicted dataset produces ρ^2 coefficients of 0.98 and 0.88 for impact force magnitude and impact width, respectively. These outcomes are encouraging, especially considering the early development phase of the impact sensor and the relatively limited number of samples used in model training.

The machine learning model was further validated for sensors printed on Cu-coated Kapton and bonded to the Kevlar strap as shown in Figure 8. The model returns ρ^2 coefficients of 0.82 and 0.80 for the impact magnitude and impact width, respectively. This dataset exhibits more variance which, is predictable due to the small sample size and less consistent sensor-substrate adhesion.

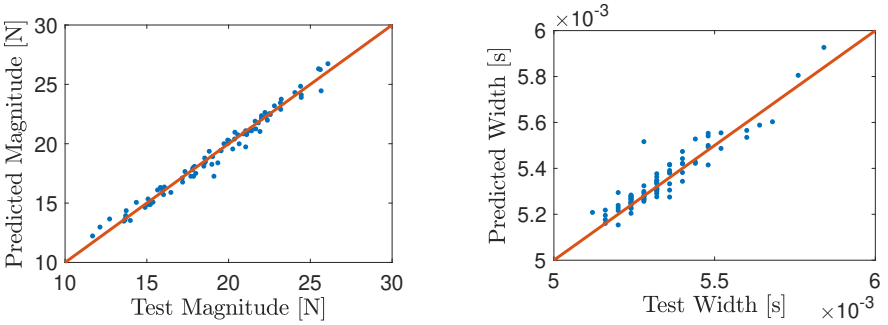

(a) Predicted impact magnitude (b) Predicted impact width

Figure 7: Impact force magnitude (a) and width (b) as predicted by machine learning model versus experimental values measured by impact hammer for the Cu dog bone sample. The line represents the ground-truth line while the scattered points represent the dataset.

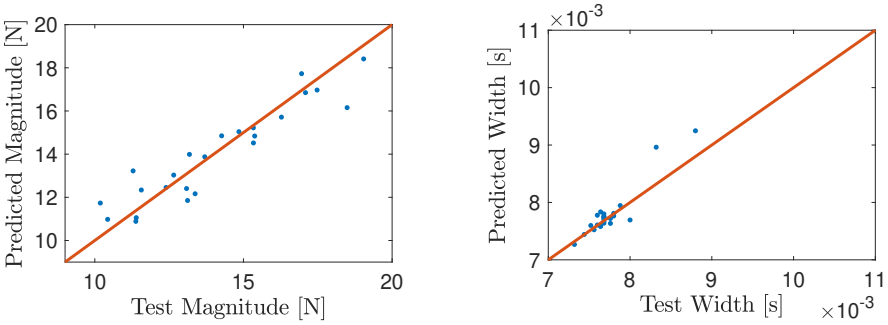

(a) Predicted impact magnitude (b) Predicted impact width

Figure 8: Impact force magnitude (a) and width (b) as predicted by machine learning model versus experimental values measured by impact hammer for the Kevlar sample bonded with Omega TT300 adhesive. The line represents the ground-truth line while the scattered points represent the dataset.

5 Conclusion

In this study, a fully printed, dual-mode sensor capable of operating in both piezoresistive and piezoelectric modes on SSTs was developed. When operating in the piezoresistive mode, the printed sensor achieved strain gauge factors of 1.41-3.68 in the low strain region and 5.64-8.02 in the high strain region, accompanied by average linear correlation coefficients of 0.93 and 0.99 respectively. The sensor accuracy was quantified by the linear correlation coefficient $/rho^2$ between results predicted by the machine learning model and the experimental results, when it is operating in the piezoelectric mode. For impact force magnitude detection, the ρ^2 values were 0.98 and 0.87, which are measured from sensors printed on Cu dog bone and Cu-coated Kapton substrates, respectively. While the ρ^2 values were 0.95 and 0.88 for impact force width prediction from sensors printed on Cu and Cu-coated Kapton, respectively. Future directions for this project include direct printing of the dual-mode sensor onto Kevlar substrates, eliminating the necessity for adhesive processes. Additionally, the deployment of a sensor network will be explored to fully leverage the capabilities of this highly versatile sensor. Further research will also investigate the use of more flexible conductive inks, enhancing the sensor's durability under larger strains and delaying gauge failure.

6 Acknowledgements

This research was supported by National Aeronautics and Space Administration under Award No 80NSSC22M0172. Z.D. would also like to acknowledge the career development support from Institutional Development Awards (IDeA) from the National Institute of General Medical Sciences of the National Institutes of Health under Grants #P20GM103408 and P20GM109095. Neither the U.S. Government nor any agency thereof, nor any of their employees, makes any warranty, expressed or implied, or assumes any legal liability or responsibility for the accuracy, completeness, or usefulness, of any information, apparatus, product, or process disclosed, or represents that its use would not infringe privately owned rights. References herein to any specific commercial product, process, or service by trade name, trademark, manufacturer, or otherwise, does not necessarily constitute or imply its endorsement, recommendation, or favoring by the U.S. Government or any agency. The views and opinions of authors expressed herein do not necessarily state or reflect those of the U.S. Government or any agency thereof.

References

[1] J. Hinkle, G. Sharpe, J. Lin, C. Wiley, and R. Timmers, "Intelligent flexible materials for space structures expandable habitat engineering development unit," 2010.

[2] D. A. Litteken, "Evaluation of strain measurement devices for inflatable structures."

[3] E. L. White, M. C. Yuen, J. C. Case, and R. K. Kramer, "Low-cost, facile, and scalable manufacturing of capacitive sensors for soft systems," *Advanced Materials Technologies*, vol. 2, 9 2017.

[4] E. Peiner, A. Tibrewala, R. Bandorf, S. Biehl, H. Lüthje, and L. Doering, "Micro force sensor with piezoresistive amorphous carbon strain gauge," *Sensors and Actuators, A: Physical*, vol. 130-131, pp. 75–82, 8 2006.

[5] A. C. Okafor, A. W. Otieno, A. Dutta, and V. S. Rao, "Detection and characterization of high-velocity impact damage in advanced composite plates using multi-sensing techniques."

[6] Y. Fujii and J. D. Valera, "Impact force measurement using an inertial mass and a digitizer," *Measurement Science and Technology*, vol. 17, pp. 863–868, 4 2006.

[7] S. Joshi, G. M. Hegde, M. M. Nayak, and K. Rajanna, "A novel piezoelectric thin film impact sensor: Application in non-destructive material discrimination," *Sensors and Actuators, A: Physical*, vol. 199, pp. 272–282, 2013.

[8] W. B. Zhu, S. S. Xue, H. Zhang, Y. Y. Wang, P. Huang, Z. H. Tang, Y. Q. Li, and S. Y. Fu, "Direct ink writing of a graphene/cnt/silicone composite strain sensor with a near-zero temperature coefficient of resistance," *Journal of Materials Chemistry C*, vol. 10, pp. 8226–8233, 5 2022.

[9] H. Nassar, G. Khandelwal, R. Chirila, X. Karagiorgis, R. E. Ginesi, A. S. Dahiya, and R. Dahiya, "Fully 3d printed piezoelectric pressure sensor for dynamic tactile sensing," *Additive Manufacturing*, vol. 71, 6 2023.

[10] J. Gomes, J. S. Nunes, V. Sencadas, and S. Lanceros-Mendez, "Influence of the -phase content and degree of crystallinity on the piezo-and ferroelectric properties of poly(vinylidene fluoride)," *Smart Materials and Structures*, vol. 19, 2010.

[11] Z. Guo, J. Xu, Y. Chen, Z. Guo, P. Yu, Y. Liu, and J. Zhao, "High-sensitive and stretchable resistive strain gauges: Parametric design and diw fabrication," *Composite Structures*, vol. 223, 9 2019.

[12] H. S. Kim, J. S. Kang, J. S. Park, H. T. Hahn, H. C. Jung, and J. W. Joung, "Inkjet printed electronics for multifunctional composite structure," *Composites Science and Technology*, vol. 69, pp. 1256–1264, 6 2009.

[13] Z. H. Tang, Y. Q. Li, P. Huang, H. Wang, N. Hu, and S. Y. Fu, "Comprehensive evaluation of the piezoresistive behavior of carbon nanotube-based composite strain sensors," *Composites Science and Technology*, vol. 208, 5 2021.